

1 **The relationship between benthic nutrient fluxes and bacterial community in Aquaculture**
2 **Tail-water Treatment Systems**

3
4 **ABSTRACT** Constructed-wetlands, Biofilms, and sedimentation are potential aquaculture tail-
5 water treatments however their roles on the distribution of benthic microbial community and the
6 way they affect the interaction between microbial community and inorganic nutrient fluxes have
7 not been fully explored. This study applied 16S rRNA high-throughput sequencing technology to
8 investigate the microbial community distribution and their link with nutrient fluxes in an
9 aquaculture tail-water bioremediation system. Results showed that bacterial community
10 compositions were significantly different in constructed-wetland and biofilm treatments ($p < 0.05$)
11 relative to sedimentation. The composition of the 16S rRNA genes among all the treatments was
12 enriched with *Proteobacteria*, *Bacteroidetes*, *Firmicutes*, and *Flavobacteria*. NMDS analysis
13 showed that the bacterial composition in constructed-wetland and biofilm samples clustered
14 separately compared to those in sedimentation. The Functional-Annotation-of-Prokaryotic-Taxa
15 analysis indicated that the proportions of sediment-microbial-functional groups (aerobic-
16 chemoheterotrophy, chemoheterotrophy, and nitrate-ammonification combined) in the constructed-
17 wetland treatment were 47%, 32% in biofilm and 13% in sedimentation system. Benthic-nutrient
18 fluxes for phosphate, ammonium, nitrite, nitrate and sediment oxygen consumption differed
19 markedly among the treatments ($p < 0.05$). Canonical correspondence analysis indicated
20 constructed-wetland had the strongest association between biogeochemical contents and the
21 bacterial community relative to other treatments. This study suggests that the microbial
22 community distributions and their interactions nutrient fluxes were most improved in the
23 constructed-wetland followed by the area under biofilm and sedimentation treatment.

24

25 **KEY WORDS:** Sediment bacteria community; Tail-water; Biofilm; Constructed-wetland;
26 Nutrients; High throughput sequencing

27

28 Regan Nicholaus^{1,2}, Betina Lukwambe^{1,3}, Wen Yanga¹, Zhongming Zheng^{1*}

29 1 School of Marine Sciences, Ningbo University, Ningbo 315832, China

30 2 Department of Natural Sciences, Mbeya University of Science and Technology, Mbeya,

31 Tanzania

32 3 Department of Food Science and Technology, University of Dar es Salaam, Dar es Salaam,

33 Tanzania

34 ***Corresponding author**

35 Email: zhengzhongming@nbu.edu.cn,

36 Mailing address: Ningbo University at Meishan, 169 Qixingnan Rd, Beilun District, Ningbo,

37 315832 China

38

39 **Introduction**

40 Intensive aquaculture farming practices have contributed overwhelming allochthonous
41 organic matter (OM), excreta, food-wastes, and dissolved nutrients (e.g., nitrogen and
42 phosphorous) with substantial impacts on the environment [1-6]. The pollution increment within
43 the environment has increased the concern for the adoption of aquaculture effluent treatments.
44 Biological effluent treatments such as constructed wetland and biofilm and physical treatments
45 like sedimentation are highly used in treating aquaculture effluents [7-9].

46 Constructed-wetlands are artificially designed biological systems consisting of a complex
47 substrate, plants (macrophytes), microbes, and water bodies forming an ecosystem [10]. Besides

48 they are a well-established, viable, suitable, and cost-effective method for treating various forms
49 of wastewater such as industrial and agricultural wastewaters [11]. Wetland plants
50 photosynthesize by their aboveground organs, while their roots and rhizospheres interact with the
51 below-sediment to drive the productivity of the heterotrophic soil biota [12, 13]. Wetland
52 rhizospheres are essentially oxic-habitats or niches created by the roots' aeration and can
53 markedly affect the diversity of the wetland's heterotrophic biota [14]. Wetlands can influence
54 water and/ or sediment physicochemical properties through different mechanisms including
55 microbial OM mineralization, sedimentation and substrate-adsorption processes [9,15].

56 Biofilms are ubiquitous and auto-aggregate forms of heterogeneous microbial communities
57 that are attached to each other and can invariably develop on solid surfaces exposed to aquatic
58 environments [16, 17]. Biofilm communities consisted of bacteria and microalgae which secrete
59 an extracellular polymeric substance matrix (polysaccharides) which facilitates the adhesion of
60 the community to other substrates. The physical nature of biofilm exopolymers has a great
61 adsorptive capacity with a super binding affinity for nutrients [17]. Biofilms can contribute
62 substantially to nutrient cycling, organic matter degradation, and community enrichment due to
63 bacteria mineralization [9,18, 19].

64 Sedimentation is the physical process by which suspended material such as clay, silts and
65 other organic particles found in the water settle by gravity. The resulting sedimentary niche at the
66 settling area could form microbial communities and nutrient-rich ecosystems [20]. Provoost et al.
67 [21] reported that sediment can harbor up to 30% of the pelagically produced organic matter.
68 Various pollutants in the water body are deposited onto the sediments and through microbial
69 waste degradation processes such as bioremediation undergo biological transformations resulting
70 in increased nutrient cycling, pollution reduction, and bacterial diversity [22-24]. Sediment

71 microorganisms like heterotrophic marine bacteria are very crucial in nutrients cycling and OM
72 processing [25].

73 The strength and efficacy of the constructed wetland and biofilm treatments are supported
74 by the consortium of bacterial communities [9, 26]. Thus, exploring the relationship between
75 biological treatment methods such as constructed wetlands and biofilms on bacterial community
76 and sediment properties is imperative. A couple of studies investigated various effluent treatment
77 systems focusing on microbial community composition and distribution [9, 19, 27]. However,
78 the impacts associated with constructed wetland, biofilm and sedimentation in response to
79 benthic properties, nutrient fluxes, and distribution of bacterial community during
80 bioremediation of aquaculture tail-water remain unclear. In this study, we aimed to (i) evaluate
81 the distribution of microorganisms in constructed wetland, biofilm, and sedimentation (ii)
82 explore the distribution of microbial functional groups among the treatments and (iii) investigate
83 the relationship between nutrient fluxes and microbial functional groups/microbial community.
84 This study will add knowledge on the distributions of sediment microbial community and
85 nutrient fluxes of an aquaculture tail-water treatment system

86 **Materials and Methods**

87 **Study area, Experimental design and Sampling**

88 The experiment was conducted in Ningbo Xiangshan Bay, Zhejiang Province, China, at a
89 land-based aquaculture tail-water treatment system constructed. This system was primarily to
90 restore effluents resulting from an intensive Commercial Vannamei Shrimp (*Litopenaeus*
91 *vannamei*) production farm. A comprehensive aquaculture tail-water treatment system composed
92 of subsystems: constructed-wetland, biofilm, and sedimentation was studied [28]. The
93 constructed-wetland subsystem was composed of emergent macrophytes, *Spartina anglica*,

94 occupying 400 sq. m of the total system area. The planting densities of *S. anglica* were 50% of
95 the total wetland cover. These plants grew rapidly to colonize the wetland and they were not
96 harvested during this study. The biofilm system was deployed with suitable aeration facilities
97 and suspended carriers in the form of fiber threads (adhesive matrix of extracellular polymeric
98 substances) for enhancing the surface area for microorganism attachment. The physical
99 sedimentation consisted of bare sediment surface, overlying aquaculture effluent water, and
100 aeration. This system was involved in filtering and settling large particles of the incoming
101 effluent water from the production center.

102 Sampling started one year after the project launched to let the ecological succession develop.
103 To ensure a representative sampling strategy, data was collected three times consecutively,
104 between April to July. Four different sampling points from each system were identified and
105 sampled. 0.5L of the overlying water was collected from each system for water quality analysis.
106 Using a handheld sediment corer four undisturbed sediment cores (8 cm height) from each
107 system were gently collected in cylindrical plastic tubes (i.d. 6.4 cm, height 19.4 cm). The
108 sediment cores and water samples were immediately brought back to the laboratory for
109 physicochemical analysis and incubation. Water samples were stored at 4°C, whereas the
110 sediment cores were kept ready for the incubation experiment.

111 The incubation experiment was done as previously described [29]. Water samples for the
112 determination of benthic flux rates for the total ammonia nitrogen (TAN), nitrate (NO₃⁻-N) and
113 nitrite (NO₂⁻-N), and soluble reactive phosphate (SRP) were collected, filtered in 0.45 GF/F and
114 stored under -20°C until analysis. After the incubation experiment, using a clean stainless steel
115 microspatula, the sediment cores were sliced into three sub-sampling points (surface 0-2 cm,
116 middle 2-4 cm, and bottom 4-8 cm). These subsamples were thoroughly homogenized and

117 divided into two portions. One portion was freeze-dried for physicochemical contents analysis
118 and the other portion was stored in clean polypropylene tubes at -20°C for the 16S rRNA
119 extraction.

120 **Analysis of physicochemical contents and nutrient flux rates**

121 The physicochemical water parameters (dissolved oxygen, temperature, and salinity) were
122 measured *in situ* during sampling using a handheld automated YSI 6000 multi-parameter probe
123 (USA). All water samples were analyzed using standard methods [30], where TAN was treated
124 with indophenol blue, NO₂⁻-N/NO₃⁻-N with the cadmium-copper reduction and the SRP were
125 treated with the ammonium molybdate/ascorbic acid method. All the concentrations of inorganic
126 nutrients were measured using a WESTCO SmartChem discrete analyzer 200 USA. Nutrient flux
127 rates (μmol m⁻²h⁻¹) and SOC were calculated from slopes of a linear regression concentration
128 against time using the equation previously described [29].

$$129 \quad Flux = \frac{\Delta C \cdot V}{A \cdot t}$$

130 Where: Flux is the nutrients or sediment oxygen fluxes (mmol m⁻²h⁻¹); ΔC (mgL⁻¹) is the change in
131 concentration of oxygen/nutrients (prior and after incubation); V (m³) the volume of overlying water;
132 A (m²), is the cross-sectional area of the incubation chamber; t (h) is the duration of incubation.

133 The sediment grain size distribution was determined using sieves with different mesh sizes
134 [31]. Briefly, grain-size parameters were conducted mechanically from oven-dried subsamples
135 using standard sieving methods for the sand content (500-63 μm) and sedigraph techniques for
136 the silt/clay fraction (<63 μm). Particle sizes (clay: <0.002, silt: <0.02, fine sand: <0.2, sand: <2)
137 were determined. Sediment OM was determined using the loss on ignition method (LOI) [32].
138 The sediment samples were freeze-dried, pulverized, and pre-weighed before being placed in a
139 muffle furnace at 475°C for 4 h. Then the samples were reweighed with the difference equals to

140 the %OM content. TOC (total organic carbon), TON (total organic nitrogen), and C/N
141 (carbon/nitrogen) ratio were analyzed commercially by using Carbon Elemental Analyzer.
142 Briefly, during pretreatment, 5g of the post-freeze-dried wet-sediment were ground using a
143 mortar into powder to pass through a 1-mm mesh sieve. Before analysis, further pretreatment
144 procedures necessary especially for TOC were done to remove the carbon dioxide by adding 1:1
145 HCl and oven-dried at 80°C, overnight to a constant weight.

146 **Extraction, amplification and MiSeq sequencing of the benthic bacterial DNA**

147 The total genomic sediment DNA extraction was performed from ~0.5g of homogenized
148 sediment samples using the PowerSoil™ DNA isolation kit (MoBio Laboratories, Inc., USA)
149 according to the manufacturer's recommendations. The extracted genomic DNA was stored at -
150 80°C until amplification. The PCR amplification conditions were according to Lukwambe *et al.*
151 [28] whereby the total genomic DNA was dissolved in 100 µl of DES, supplied with the kit. The
152 DNA quality and/or quantity of the samples were measured using a spectrophotometer
153 (NanoDrop Technologies Inc., Wilmington, DE, USA) at the A260/A280 ratio. A combination
154 of reverse primer (5'-GGACTACHVGGGTWTCTAAT-3') and a forward primer (5'-
155 CCTACGGGAGGCAGCAG-3') for the hypervariable V3-V4 regions of the 16S rRNA gene
156 was used. 5 µl of the total DNA template was used and amplified in a 50-µl reaction system.
157 Then the amplification process followed 30 cycles of 95°C denaturation for 30 s, annealing
158 (55°C, 30 s), and extension (72°C, 45 s) and a final extension for 5min at 72°C. Successful
159 amplification product and size of the PCR was electrophoresed in 1% agarose gel. The triplicate
160 amplified products of each sample were pooled, purified, equilibrated, and sequenced in an
161 Illumina MiSeq high-throughput sequencing platform.

162

163 **Bioinformatics analysis**

164 The sequencing process of the paired reads was initially joined with FLASH using default
165 settings [33], then, the Raw FASTQ files were processed using Quantitative-Insights-Into-
166 Microbial-Ecology (QIIME version 1.8.0, [34]. The operational taxonomic units (OTUs)
167 assigned at a 97% similarity cut-off point in all samples were clustered using USEARCH
168 (version 7.1, <http://drive5.com/uparse/>). The sequences were quality filtered based on sequence
169 length, quality score, chimera, and primer mismatch thresholds. In a nutshell, homopolymer runs
170 exceeding 6 bp were screened-out by PyroNoise. Sequences with the same barcodes were
171 assigned to the same sample. The phylotypes were performed using the UCLUST algorithm [35].
172 The most abundant sequences of each phytotype were selected as the clean sequence and were
173 taxonomically assigned (Greengenes database, release 13.8) using PyNAST [36]. Diversity
174 indices (Shannon index, Simpson, Chao1, and observed OTUs) were performed using the
175 phylogenetic tree (QIIME pipeline).

176 **Statistical analyses**

177 The variations of the different physicochemical variables were analyzed by a one-way or
178 two-way repeated ANOVA. Post Hoc tests were performed to determine the significant groups.
179 The normal distribution and homogeneity of variances among treatments were verified before the
180 ANOVA test. All the data were Hellinger transformed post statistical analyses, and then
181 normalized by using the function decostand/p-p plot in the “vegan” package to improve
182 normality and homoscedasticity. Permutational multivariate analysis of variance-
183 PERMANOVA (Bray-Curtis dissimilarity matrices) [37], phyloseq v1.22.3 and Nonmetric
184 Multidimensional Scaling (NMDS) was performed to analyze the microbial community
185 composition among the treatments. One-way analysis of similarity (ANOSIM) was used to

186 verify whether the distribution of different samples visualized in the NMDS plot was significant
187 [38]. Canonical correspondence analysis (CCA) was used to analyze the correlations between
188 bacterial community compositions and environmental variables.

189 The sediment microbial functional groups were predicted by using the Functional
190 Annotation of Prokaryotic Taxa (FAPROTAX) database. According to Louca *et al.* [39], the
191 annotated bacterial OTU table from the Silva database was read, and the data was matched with
192 the species information in the database using a python program. The predicted functions were
193 outputted through FAPROTAX (<http://www.ehbio.com/ImageGP/>). The annotation results were
194 used to describe the microbial functional compositions and abundance of related metabolic
195 pathways involved in ammonification, denitrification, carbohydrate metabolism, aromatics
196 degradation, and nitrogen fixation. The relative abundances of the functional groups were
197 calculated as the cumulative abundance of OTUs assigned to each functional group, which was
198 obtained by standardizing the cumulative abundance of OTUs correlated with at least one
199 function. All statistical analyses were performed with R, (version, 3.6.1) [40] and the results of
200 the statistical tests were considered to be significant at $p \leq 0.05$. The figures were drawn with R
201 and OriginPro 8.0 software. **Data deposition:** The sequences used in this study have been
202 deposited in the GeneBank of NCBI with the BioProject database ID PRJNA593691
203 (<https://www.ncbi.nlm.nih.gov/sra/PRJNA593691>) and SRA accession numbers ranging from
204 SAMN13483434 to SAMN13483469.

205 **Results**

206 **Sediment and water physicochemical contents**

207 The sediment physicochemical contents are described in Table 1. The results indicate
208 distinct differences in sediment organic and inorganic contents among the systems. The surface

209 sediments of the constructed-wetland consisted of 79% medium sand, 17% very fine sand, and
 210 4% silt/clay whereas the compositional contents in the biofilm were 68% medium sand, 25%
 211 very fine sand, and 7% silt. The sedimentation system was dominated by 84% (medium sand),
 212 11% (very fine sand), and 5% (silt). Cores from the sedimentation system had significantly
 213 higher contents of OM, TN, TP, TOC, and C/N ratio at all three depths (0-2 cm, 2-4 cm, and 4-8
 214 cm), relative to the others. C/N ratio were 8.17 ± 1.5 (biofilm), 7.7 ± 1.6 , (constructed-wetland) and
 215 12.32 ± 3.1 (sedimentation) on average. Total OM was much lower in biofilm (depth 0-2 cm)
 216 compared to constructed-wetland and sedimentation. All sediment organic contents varied
 217 differently between the systems however no stable variational trends were observed within
 218 different depths of the same treatment (Table 1, $p > 0.05$).

219 Table 1. Mean (\pm SD) values of the sediment organic contents among the treatments
 220 (Constructed-wetland, Biofilms, and Sedimentation). OM represents organic matter, TN: Total
 221 nitrogen, TP: Total phosphorus, TOC: Total organic carbon and C/N: Carbon to nitrogen ratio

System	Depth (cm)	OM%	TN%	TP%	TOC%	C/N
CW	Surface	3.13 ± 0.14	0.48 ± 0.05	0.031 ± 0.061	2.94 ± 0.06	6.12 ± 1.31
	Middle	3.23 ± 0.11	0.38 ± 0.02	0.029 ± 0.053	3.13 ± 0.03	8.24 ± 1.05
	Bottom	3.07 ± 0.08	0.30 ± 0.12	0.021 ± 0.006	2.63 ± 0.04	8.77 ± 2.09
BF	Surface	1.57 ± 0.05	0.43 ± 0.03	0.086 ± 0.04	3.10 ± 0.06	7.21 ± 0.81
	Middle	2.55 ± 0.04	0.41 ± 0.01	0.081 ± 0.03	3.07 ± 0.02	7.49 ± 3.32
	Bottom	3.47 ± 1.02	0.22 ± 0.01	0.952 ± 0.02	2.16 ± 0.08	9.82 ± 3.74
SD	Surface	4.79 ± 0.26	0.16 ± 0.01	0.263 ± 0.01	2.31 ± 0.06	14.43 ± 5.64
	Middle	4.12 ± 0.24	0.21 ± 0.01	0.289 ± 0.041	2.33 ± 0.25	11.09 ± 4.81
	Bottom	3.98 ± 0.31	0.26 ± 0.12	0.204 ± 0.025	2.98 ± 0.22	11.46 ± 6.06

222 **Nutrients flux rates among the treatments**

223 All dissolved inorganic nutrient flux rates showed an efflux trend among the treatments. The
224 mean release rates of TAN, NO₃⁻-N, NO₂⁻-N, and SRP fluxes between biofilm, constructed-
225 wetland, and sedimentation cores were significantly different (2-way ANOVA, p<0.05). NO₂⁻-N
226 and TAN accounted for more than 87.51% (constructed-wetland) and 71.14% (biofilm) net flux
227 rate relative to 37.43% (sedimentation) (Fig 1). The NO₃⁻-N flux rates were 396.15±61.09 μmol
228 m⁻²h⁻¹ (constructed wetland), 249.83±71.12 μmol m⁻²h⁻¹ (biofilm), 173.7±33.01 μmol m⁻²h⁻¹,
229 (sedimentation) (Fig 1B). The constructed wetland had the highest exchange rate of NO₃⁻-N, and
230 NO₂⁻-N relative to other systems (biofilm and sedimentation). The SRP had the highest mean
231 flux rate in biofilm. The release rate of TAN into the overlying water (constructed-wetland) was
232 approximately twice higher in both biofilm and sedimentation, indicating sedimentary
233 remineralization of ammonia and nitrate. SOC were 4.91±0.75 mmol m⁻²h⁻¹ (biofilm), 3.82±0.37
234 mmol m⁻²h⁻¹ (constructed wetland), 1.89±0.31 mmol m⁻²h⁻¹ (sedimentation) (Fig 1A). Oxygen
235 level in sedimentation subsystem was the lowest followed by constructed wetland and finally
236 biofilm. Generally, the mean release rates of all nutrient groups including soc followed the order:
237 biofilm>constructed wetland>sedimentation.

238

239 **[Fig 1]**

240 **Microbial community composition and structure**

241 The bacterial community compositions varied among depths and between the treatment
242 systems (Fig 2). A total of 519, 692, and 837 OTUs were identified for sedimentation,
243 constructed-wetland, and biofilm treatments respectively. Jointly the OTUs represent 54 phyla,
244 85 classes, 152 families, and 471 genera among all treatments. The relative content of the
245 microbial community (>0.3% relative abundance) at phylum, class, and family level is illustrated

246 (Fig 2A-C). At the phylum level, *Proteobacteria* were the most dominant community in all three
247 systems accounting for $32.17 \pm 7.51\%$, followed by *Bacteroidetes* ($29.32 \pm 7.04\%$), *Chloroflexi*
248 ($20.65 \pm 6.21\%$), *Actinobacteria* ($19.44 \pm 5.92\%$), *Firmicutes* ($13.92 \pm 4.09\%$), *Acinetobacter*
249 ($11.85 \pm 3.71\%$) and *Planctomycetes* ($8.83 \pm 2.54\%$) (Fig. 2A). The phylum *Firmicutes* and
250 *Proteobacteria* were most dominant in constructed wetland and biofilm, while the sedimentation
251 community was mainly dispersed by *Firmicutes*, *Proteobacteria*, and *Bacteroidetes*. *Gamma-*,
252 *Delta-*, and *Alpha-proteobacteria* were dominant classes in all systems, followed by
253 *Anaerolineae*, *Actinobacteria*, *Cytophagia*, and *Flavobacteriia* (Fig 2B). Further, at the family
254 level, several predominantly expressed bacterial taxa (*Clostridiaceae* and
255 *Acidaminobacteraceae*, (Order-*Clostridiales*), *Rhodobacteraceae* (Order-*Rhodobacterales*)
256 *Chloroflexi*, *Anaerolineaceae*, [*Thermodesulfobivibrionaceae*] (order-*Nitrospirales*) were
257 predominant in all three treatments (Fig 2C). The family *Flavobacteriaceae* was highly
258 distributed in biofilm (15 to 65-fold) relative to constructed-wetland (9-31-fold) and
259 sedimentation (7-17-fold). Other families were *Nitrospiraceae* and *Planctomycetaceae* with a
260 20-50-fold higher (biofilm) relative to constructed-wetland and sedimentation (jointly 6-12-fold).
261 The distribution of the most dominant bacterial community (at the genera level) among the
262 treatments is represented by heatmap (Fig 3). The heatmap includes the top thirty genera, which
263 represent 94.2-97.5% of all 16S rRNA bacterial genes reads. The *Disulvococcus*,
264 *Novosphingomium*, *Fusibacteria*, *Kordia*, *Clostridium*, and *Lysobacter* were the genera highly
265 distributed among the treatments (Fig 3; 0-4 cm depth). Vertically, the proportions of
266 *Proteobacteria*, *Acidobacteria*, and *Bacteroidetes* were high in surface sediments, whereas
267 *Chloroflexi* and *Firmicutes* tended to be enriched in deep layers.
268

269 **[Fig 2]**

270 **Diversity of bacterial community among the systems**

271 The bacterial community differed significantly among the treatments (ANOSIM, $p = 0.031$).
272 The microbial community richness estimate (Chao1) ranged from 7321 to 9531 sequences
273 (biofilm), 4637 to 9017 (constructed-wetland), 6214 to 8973 (sedimentation). Biofilm had
274 significantly Chao1 values ($p < 0.05$) and constructed-wetland had the highest bacterial diversity
275 (Shannon index values). Bacterial richness estimates were highest and most diverse at the surface
276 sediments (0-2 cm) and dropped with a depth increase (Fig 3). The Shannon index ranged from
277 6.79 (surface), 6.03 (middle) to 5.81 (bottom) in biofilm samples and 6.21 (surface), 6.05
278 (middle), 4.93 (bottom) in constructed-wetland samples whereas sedimentation ranged from 5.06
279 (surface), 3.5 (middle), 2.53 (bottom). The diversity trend order was constructed-
280 wetland>biofilm>sedimentation. Moreover, the NMDS ordinations assessment revealed marked
281 differences in community composition grouping patterns between the systems, and between
282 depths (Fig 4). The samples were grouped separately within depths and between treatments. The
283 microbial community in constructed-wetland treatment samples was more clearly separated
284 suggesting the highest species dissimilarity compared to other treatments. PERMANOVA
285 further confirms that bacterial community composition between the treatments and within depth
286 groups was significantly different (Table 2: $p < 0.05$).

287

288

289 Table 2. 16S rRNA sediment microbial community distributions, structure, and composition
290 determined by a permutational multivariate analysis of variance (PERMANOVA, Adonis
291 function) among the treatments.

292

293

	Sums of Sqs	Means Sqs	F. Model	R²	P
Groups	3.0131	1.73516	7.7641	0.29737	0.000*
Depth	0.9362	0.58454	4.5153	0.34574	0.003*
Groups*Depth	0.1795	0.30134	1.9438	0.03952	0.042*

294

295

[Fig 3]

296

297

[Fig 4]

298 **Microbial community and environmental variables**

299 To explore the relationship between the sediment-microbial community and environmental
300 factors, a correlation analysis was performed based on CCA. The analysis showed significant
301 correlations between microbial community composition (genus level) and the environmental
302 factors (Mantel test, $p < 0.05$). The CCA showed the two components of the graph jointly
303 explained 78.89% (axis 1: 41.37% and axis 2: 29.52%) of the total sediment microbial
304 community variance, implying that physicochemical factors and bacterial community
305 composition/structure had a substantive influence over the other. Generally, nine environmental
306 variables were significantly associated with the bacterial community among the treatments (Fig
307 5). The weakest correlation was observed between SRP and $\text{NO}_2\text{-N}$ and the communities
308 (sedimentation). A significant correlation between *Desulphobacterales*, *Nitrospira*, and
309 *Clostridia* taxa and the variables TN, TOC, and TP were evident. Significant correlations
310 between *Nitrospira* and TOC, TN, and SRP (biofilm) and TAN in the constructed-wetland
311 samples were observed. Furthermore, significant correlations between *Desulfomicrobium*,
312 *Cytophagales*, and *Planctomyces* and $\text{NO}_2\text{-N}$, and TP in the sedimentation samples were found.

313 Whilst *Ferimonas* and *Verrucomicrobium* were positively correlated with TOC, *Burkholderiales*
314 positively correlated with TAN, TP, and SRP especially in the constructed-wetland samples (Fig
315 5).

316 [Fig 5]

317 Sediment microbial functional groups distributions

318 Using FAPROTAX the analysis revealed a comparative number of various specific
319 metabolic functional groups/pathways (e.g., chemo-heterotrophy, nitrate-ammonification,
320 nitrification, denitrification, Fig 6) associated with the 16S rRNA genes. Different functional
321 groups involved in nitrogen transformation pathways especially in the surface (0-2 cm) and
322 middle (2-4 cm) cores were predicted suggesting elevated nitrogen mineralization activities. The
323 relative abundance of genes mediating denitrification and dissimilatory reduction of nitrate to
324 ammonia were mostly higher in the bottom layers (4-8 cm) in all systems. Chemoheterotrophy
325 (29.73±0.11%) was the main metabolic functional group, followed by denitrification (23.51±
326 0.03%), and complete nitrification (15.05±0.81%). Other promoted functional groups/pathways
327 included aerobic-chemoheterotrophy, sulfate_respiration, nitrate_ammonification, and
328 nitrite_ammonification, especially in biofilm cores. Of all functional groups, groups related to
329 nitrogen-cycling were highly predicted in the constructed-wetland relative to biofilm and
330 sedimentation samples.

331 [Fig 6]

332 Discussion

333 Biofilm, constructed wetland, and sedimentation are potential treatments for improving
334 wastewater and sediment quality [9, 8]. This treatment can improve the ecosystem processes
335 including sediment microbial community activities, distribution, structure, abundance, and
336 successions. The availability and distribution of bacterial communities in the sediment can help

337 to improve and optimize the bioremediation process [8, 41, 42]. This study indicates that a
338 couple of ecological activities including microorganism distribution patterns, nutrient dynamics,
339 and contents of the OM were significantly influenced by the treatments

340 **Microbial community composition and distribution**

341 The sedimentary bacterial community compositions and structure among the treatments
342 were differently distributed (Figs 3, 4; Table 2). Biofilm and constructed wetland treatments
343 supported more abundant and distinct microbial communities especially at the surface layers (Fig
344 2). Particularly, phyla such as Proteobacteria and Acidobacteria were most abundantly
345 distributed across all samples, with the highest relative abundance been recorded in biofilm
346 samples relative to constructed-wetland and sedimentation suggesting an elevated mineralization
347 hence nutrient fluxes (Fig 1). This suggests that the treatments probably created varying
348 ecological conditions that accelerate microbial activities and multiplication. The *Proteobacteria*,
349 *Bacteroidetes*, *Acidobacteria*, *Deltaproteobacteria*, *Clostridia*, *Firmicutes*
350 *Gammaproteobacteria*, and *Bacilli* were among the most dominant phyla with approximately
351 37% and 43% bacterial composition in constructed-wetland and biofilm respectively compared
352 sedimentation (19%) (Fig 4). Some studies suggest that soil microbial distribution can be
353 regulated by the different vegetation types [43, 44]. In this study, microbial diversity was highly
354 distributed especially within the constructed-wetland subsystem (Figs. 2A-C, 3). Bodelier, [45]
355 and Lukwambe *et al.* [9] wetland rhizospheres are oxic-habitats created by the roots' aeration
356 and can markedly affect the diversity of the wetland's heterotrophic biota and activate nutrient
357 fluxes.

358 There is a substantial interaction among the constructed wetland plants, microorganisms,
359 and contaminants supported by their complex rhizosphere system [46]. Besides, the plants roots

360 forming the constructed-wetland harbor/store useful nitrifying-denitrifying bacteria [47]. This is
361 evident especially with the rhizosphere of emergent aquatic plants, where the plant roots provide
362 a favorable habitat and exudate the growth of various microbes responsible for sediment
363 reworking including sediment nitrogen content transformation [48, 49]. A profound number of
364 *Proteobacteria*, *Chloroflexi*, and *Acidobacteria*, were observed within the biofilm and
365 constructed wetland, this may suggest the presence of elevated mineralization activities which
366 affect the succession and stability of the bacterial community [50, 51, 52]. Also, a biofilm
367 environment can potentially improve bacterial communities distributions [53]. Based on this
368 observation, we can deduce that both biofilms and constructed wetlands favored more bacterial
369 community related to organic wastes degradation relative to other sedimentation systems.

370 Its known remediation measures by using constructed-wetland, biofilm, and sedimentation
371 are known to influence the aquatic ecosystem biodiversity due to improved sediment conditions
372 [29]. The sedimentary ecological niches created by each system differently affect the biotic and
373 abiotic characteristics, thereby resulting in the change of the aquatic microbial diversity and
374 functional diversity [54].

375 **Biogeochemical fluxes and functional microbial community**

376 In the current study, constructed-wetland showed higher SRP, NO₂⁻-N, NO₃⁻-N, and TAN
377 flux rates relative to other treatments (Fig 1). This release pattern is ascribed to promoted
378 physicochemical-microbial mediated activities such as mineralization, nitrification-
379 denitrification, and redox reaction [8, 19]. Literatures show that the root system of the
380 constructed-wetland plants has rhizomes that aerate the sediment potentially resulting in
381 increased dissolved oxygen which promotes microbial assemblages and nitrification-
382 denitrification activities [9, 55, 56]. In this study, we found several bacterial taxa associated with

383 ammonium oxidizing bacterial (AOB, e.g., *Nitrospira*) and nitrite-oxidizing bacteria (NOB,
384 *Nitrospina*, *Nitrosomonas*) and sulfate-reducing bacteria (SRB, *Desulfatibacillum* and
385 *Desulfobacterium*) which contribute to effluent degradation and material transformation [26, 56].
386 These species were enriched in both constructed wetland and biofilm indicating that the elevated
387 nutrient fluxes were probably due to enhanced bacterial activities such as organic matter
388 mineralization. On the other hand, putatively performing dissimilatory nitrate reduction to
389 ammonia taxa were about 2.5- to 3-fold more in biofilm and constructed-wetland suggesting an
390 increased mineralization activity including nitrification. Normally nitrification process is
391 facilitated by both AOB and NOB bacterial [57]. Under the presence of oxygen microbial
392 nitrogen transformation is supported. Vila-Costa *et al.* [58] reported that macrophyte species
393 with high root oxygen release capacity may enhance the diversity and activity of ammonia
394 oxidizers leading to increased nitrogen content transformation.

395 Lower TAN fluxes were observed in the biofilm treatment system suggesting increased
396 ammonia utilization by nitrifying bacteria such as *Nitrosomonas* and *Nitrobacter*. These group of
397 bacterial are reported to reduce excess nitrogenous content in the sediment [19]. In our study,
398 several bacterial functional groups related to biogeochemical nutrient metabolism, cycling, and
399 degradation were discovered (Fig 6). The expression of chemoheterotrophy, aerobic-
400 chemoheterotrophy, and denitrification microbial functional groups was significantly higher in
401 the constructed wetland than biofilm and sedimentation. This implied that constructed-wetland
402 best enhanced the activities related to effluent degradation that led to increased nutrient
403 transformation and fluxes. This as well suggests that the genes associated with different
404 biogeochemical functions were favored and enhanced. Sediment nitrogen fixation, nitrification,
405 denitrification, ammonification, and other major nitrogen transformation processes are mediated

406 by soil bacteria [56, 59]. The sedimentary nitrogen cycle can be improved by biological
407 nitrification and denitrification pathways leading to healthy environmental ecosystems. For
408 example, we observed an increase in the absolute content of functional group related
409 *Acinetobacter* (*Moraxellaceae*), which is responsible for detoxification of different pollutants,
410 such as degradation of aromatic compounds [60]. The increased SRP flux rate from the sediment
411 into the water (biofilm, Fig. 1B) indicates organic matter transformation could have been
412 promoted by the bacterial community. Ki *et al.* [56] indicated that organic wastes can be
413 decomposed into soluble reactive phosphate by the SRB bacteria, such as *Desulfobacterium*,
414 *Desulfatibacillum*, *Desulfomicrobium*, and *Desulfosalsimonas*, which were most evident in both
415 biofilm and constructed-wetland.

416 **Bacterial community and sediment organic contents**

417 The content of TON, TOC, TP, and TOM varied significantly among the treatments (Table
418 1). The observed distribution trend was likely due to improved bacterial community activities
419 associated with mineralization, such as nitrification-denitrification. Sediment nitrogen fixation,
420 nitrification, denitrification, ammonification, and other major nitrogen transformation processes
421 are mainly mediated by soil bacteria [59]. The expression of *Dechloromonas*, *Steroidobacter*,
422 and *Novosphingobium* among the treatments are likely to support the denitrification process and
423 strengthen the physicochemical-microbial interactions. For instance, *Dechloromonas* has been
424 described as denitrifiers that produce nitrogen gas as a reduced nitrogen product [61]. Fabian *et al.*
425 [62] stated that denitrification can also be fueled by the presence of *Steroidobacter* in the
426 sediments. Generally, the lower TN and OM in biofilm and constructed wetland over the
427 sedimentation is probably due to the TAN transformation through microbial oxidation to NO_3^- -N
428 and NO_3^- -N. The majority of nitrogen content reduction in wetlands is believed to result from the

429 microbial coupled nitrification-denitrification interactions and uptake by the wetland plants [63].
430 The 16S rRNA sequencing result showed that taxa such as *Firmicutes* and *Nitrospinae* were
431 differentially enriched among the treatments a phenomenon that may have attributed to the
432 reduced level of the organic contents.

433 Additionally, CCA indicated strong relationships between the bacterial communities and
434 physicochemical factors (Fig 5). Among the treatments, nine environmental variables (TAN,
435 NO₂⁻-N, NO₃⁻-N, SRP, TN, TP, TOC, OM and, SOC) correlated more closely with microbial
436 community groups. The correlations between bacterial communities and nutrient fluxes and
437 organics were moderately high (ordination axis 1 = 58.1%, axis 2 = 42.7% of the total variation).
438 The constructed-wetland and biofilm had more affiliated taxa linked with physicochemical
439 variables relative to sedimentation indicating a greater association between the functional genera
440 among the two treatments. This result is similar to Wu *et al.* [64], Lukwambe *et al.* [29] and Ki
441 *et al.* [56] who reported a substantial correlation among the bacteria and nitrogen transformation.
442 In similar patterns, CCA results revealed that TAN, TP, TOC, and TN contents were factors that
443 strongly correlated with *Desulfomicrobium* (surface sediment) and *Chloroflex* (deeper sediment,
444 biofilm) while SOC, TP, and SRP mostly correlated with *Ferrimonas*, *Burkholderia*,
445 *Dechloromonas*, and *Desulfomicrobium*, especially in constructed-wetland. This can be
446 supported by a previous study [56, 65] which indicated *Desulfomicrobiuim* and *Methylobacter*
447 had strong association with TAN resulting in reduced organic contents.

448 **Conclusions**

449 This study investigates the distributions of the bacterial community, nutrient-fluxes, and
450 organic matter contents in a comprehensive aquaculture tail-water treatment system. The study
451 showed that the treatments differently improved the sediment bacterial dynamics (community

452 structure, diversity, and composition), elevated nutrient dynamics and fluxes, and reduced
453 organic matter contents. Microbial groups associated with AOB, NOB, SRB were enriched in the
454 constructed wetland and biofilm but so within the 0-4 cm sediment depth. The
455 chemoheterotrophy, aerobic-chemoheterotrophy, denitrification, and nitrification were the most
456 dominant functional groups of all treatments but especially in the constructed wetland. The TAN,
457 NO_2^- -N, and NO_3^- -N nutrient flux rates across the sediment-water interface were higher in
458 constructed-wetland than in biofilm and sedimentation subsystems. The constructed-wetland and
459 biofilm had lower organic effluents and better sediment conditions relative to sedimentation. Our
460 study suggests that bacterial diversity and structure were highly improved especially under
461 constructed-wetland. Whereas biofilm best promoted the bacterial community composition
462 relative to other treatments.

463 **Acknowledgments**

464 This study was supported by National Key R & D Program of China (2020YFD0900201), the
465 Zhejiang Public Welfare Technology Research Program of China (ZPWTP) (LGN18C190008)
466 and the K.C. Wong Magna Fund in Ningbo University

467

468 **References**

- 469 1. Kalantzi I, Karakassis I. Benthic impacts of fish farming: meta-analysis of community
470 and geochemical data. *Mar. Pollut. Bull.* 2006; 52:484-493.
- 471 2. Cabello FC. Heavy use of prophylactic antibiotics in aquaculture: a growing problem for
472 human and animal health and for the environment. *Environ Microbiol.* 2006; 8:1137-
473 1144.
- 474 3. Roeselers G, Loosdrecht MC, M van Muyzer G. Phototrophic biofilms and their potential
475 applications. *J Appl Phycol.* 2007; 20(3): 227-235. Abatenh E, Gizaw B, Tsegaye Z,

- 476 Wassie M. The Role of Microorganisms in Bioremediation- A Review. OJEB. 2017; 2(1):
477 038-046.
- 478 4. Dean RJ, Shimmield TM, Black KD. Copper, zinc and cadmium in marine cage fish farm
479 sediments: an extensive survey. Environ Pollut. 2007; 145:84-95.
- 480 5. Basaran AK, Aksu M, Egemen O. Impacts of the fish farms on the water column nutrient
481 concentrations and accumulation of heavy metals in the sediments in the eastern Aegean
482 Sea (Turkey). Environ Monit Assess. 2010; 162:439-51.
- 483 6. Martinez-Porchaz M, Martinez-Cordova LR. World aquaculture: Environmental impacts
484 and troubleshooting alternatives. Sci. World J. 2012; 389623
- 485 7. Brito LO., Cardoso Junior L, de O, Lavander HD, Abreu JL, de Severi W, Gálvez AO.
486 Bioremediation of shrimp biofloc wastewater using clam, seaweed, and fish, Chem Ecol .
487 2018; 1-13
- 488 8. Nicholaus R, Lukwambe B, Lai H, Yang W, Zheng Z Nutrients cycling in ecological
489 aquaculture wastewater treatment systems: vertical distribution of benthic phosphorus
490 fractions due to bioturbation activity by *Tegillarca granosa*. Aquaculture Environ Interact.
491 2019a; 11: 469-480.
- 492 9. Lukwambe B, Zhao L, Nicholaus R, Yang W, Zhu J, Zheng Z. Bacterioplankton
493 community in response to biological filters (clam, biofilm, and macrophytes) in an
494 integrated aquaculture wastewater bioremediation system. Environ. Pollut. 2019; 254
495 113035.
- 496 10. Kivaisi AK. The potential for constructed wetlands for wastewater treatment and reuse in
497 developing countries: a review, Ecol Eng. 2001; 16(4): 545-560.

- 498 11. Webb JM, Quinta R, Papadimitriou S, Norman L, Rigby M, Thomas DN, Le Vay L.
499 Halophyte filter beds for treatment of saline wastewater from aquaculture. *Water Res.*
500 2012; 46:5102-5114.
- 501 12. Neori A, Agami M. The Functioning of Rhizosphere Biota in Wetlands- a Review.
502 *Wetlands.* 2016; 37(4): 615-633.
- 503 13. Bonkowski M, Villenave C, Griffiths B. Rhizosphere fauna: the functional and structural
504 diversity of intimate interactions of soil fauna with plant roots. *Plant Soil.* 2009; 321:
505 213-233.
- 506 14. Bodelier PLE. Interactions between oxygen-releasing roots and microbial processes in
507 flooded soils and sediments. In: de Kroon H, Visser EJW (eds) *Root ecology. Ecological*
508 *studies* Vol. 168. Springer-Verlag Berlin Heidelberg, Germany. 2003; 331-362
- 509 15. Kadlec RH, Knight RL. *Treatment Wetlands*, Lewis publisher, New York, NY, USA.
510 1996
- 511 16. Rao TS, Rani PG, Venugopalan VP, Nair KVK Biofilm formation in a freshwater
512 environment under photic and aphotic conditions. *Biofouling.* 1997; 11:265-282.
- 513 17. Sanz-Lázaro C, Navarrete-Mier F, Marín A. Biofilm responses to marine fish farm
514 wastes. *Environ Pollut.* 2011; 159(3), 825-832.
- 515 18. Baldwin DS, Mitchell AM, Rees GN, Watson GO, Williams JL. Nitrogen processing by
516 biofilms along a lowland river continuum. *River Res Appl.* 2006; 22: 319-326
- 517 19. Nicholas R, Lukwambe B, Zhao L, Yang W, Zhu J, Zheng Z Bioturbation of blood clam
518 *Tegillarca granosa* on benthic nutrient fluxes and microbial community in an aquaculture
519 wastewater treatment system. *Int. Biodeterior. Biodegradation.* 2019b; 142:73-82.

- 520 20. Freel KC, Edlund A, Jensen PR Microdiversity and evidence for high dispersal rates in
521 the marine actinomycete *Salinispora pacifica*. Environ. Microbiol. 2012; 14:480-93.
- 522 21. Provoost P, Braeckman U, Van Gansbeke D, Moodley L, Soetaert K, Middelburg JJ, Jan
523 Vanaverbeke J. Modelling benthic oxygen consumption and benthic-pelagic coupling at a
524 shallow station in the southern North Sea. Estuar. Coast. Shelf Sci. 2013; 120: 1-11.
- 525 22. Abatenh E, Gizaw B, Tsegaye Z, Wassie M. The Role of Microorganisms in
526 Bioremediation- A Review. OJEB. 2017; 2(1): 038-046.
- 527 23. Nicholaus R, Lukwambe B, Yang W, et al. In situ Assemblies of Bacteria and Nutrient
528 Dynamics in Response to an Ecosystem Engineer, Marine Clam *Scapharca subcrenata*,
529 in the Sediment of an Aquaculture Bioremediation System. J Ocean Univ. Chin. 2020a;
530 19: 1447–1460
- 531 24. Nicholaus R, Lukwambe B, Mwakalapa EB, Yang W, Zhu J, Zheng Z. Impacts of
532 bioturbation by Venus clam *Cyclina sinensis* (Gmelin, 1791) on benthic metabolism and
533 sediment nutrient dynamics in a shrimp-clam polyculture pond. Indian Journal of
534 Fisheries Science. 2020b. 167(3):29-38
- 535
- 536 25. Vega Thurber R, Willner-Hall D, Rodriguez-Mueller B, Desnues C, Edwards RA, Angly
537 F, Dinsedimentale E, Kelly Forest Rohwer L. Metagenomic analysis of stressed coral
538 holobionts. Environ Microbiol. 2009; 11(8):2148-63.
- 539 26. Soares-Castro P, Yadav TC, Viggior S, Kivisaar M, Kapley A, Santos PM Seasonal
540 bacterial community dynamics in a crude oil refinery wastewater treatment plant. Appl.
541 Microbiol. Biotechnol. 2019; 103:9131-9141.

- 542 27. Akyon B, Stachler E, Wei N, Bibby K. Microbial Mats as a Biological Treatment
543 Approach for Saline Wastewaters: The Case of Produced Water from Hydraulic
544 Fracturing. *Environ Sci Technol.* 2015; 49(10): 6172–6180.
- 545 28. Lukwambe B, Yang W, Zheng Y, Nicholaus R, Zhu J, Zheng Z. Bioturbation by the
546 razor clam (*Sinonovacula constricta*) on the microbial community and enzymatic
547 activities in the sediment of an ecological aquaculture wastewater treatment system.
548 *Sci. Total Environ.* 2018; 643: 1098-1107
- 549 29. Nicholaus R, Zheng ZM. The effects of bioturbation by the Venus clam *Cyclina sinensis*
550 on the fluxes of nutrients across the sediment-water interface in aquaculture ponds.
551 *Aquac Int.* 2014; 22(2):913-924.
- 552 30. APHA. Standard methods for the examination of water and wastewater, 22nd edition
553 edited by Rice EW, Baird, RB, Eaton, AD and Clesceri LS, American Public Health
554 Association (APHA), American Water Works Association (AWWA) and Water
555 Environment Federation (WEF), Washington, DC, USA; 2012
- 556 31. Giles H, Pilditch CA, Nodder SD, Zeldis JR, Currie K. Benthic oxygen fluxes and
557 sediment properties on the northeastern New Zealand continental shelf. *Cont. Shelf Res.*
558 2007; 27(18): 2373-2388.
- 559 32. Heiri O, Lotter AF, Lemcke G Loss on ignition as a method for estimating organic and
560 carbonate content in sediments: reproducibility and comparability of results. *J.*
561 *Paleolimnol.* 2001; 25: 101-110.
- 562 33. Magoč T, Salzberg SL FLASH: fast length adjustment of short reads to improve genome
563 assemblies. *Bioinformatics.* 2011; 27:2957-2963.

- 564 34. Caporaso JG, Bittinger K, Bushman FD, DeSantis TZ, Andersen GL, Knight R. PyNAST:
565 a flexible tool for aligning sequences to a template alignment. *Bioinformatics*. 2010; 26:
566 266-267.
- 567 35. Edgar RC. UPARSE: highly accurate otu sequences from microbial amplicon reads. *Nat*
568 *Methods*. 2013; 10: 996-998.
- 569 36. DeSantis TZ, Hugenholtz P, Keller K, Brodie EL, Larsen N, Piceno YM, Phan R,
570 Andersen GL. NAST: a multiple sequence alignment server for comparative analysis of
571 16S rRNA genes. *Nucleic Acids Res*. 2006; 34: 394-399
- 572 37. Anderson MJ. A new method for non-parametric multivariate analysis of variance.
573 *Austral Ecol*. 2001; 26:32-46.
- 574 38. Legendre P, Legendre L Numerical ecology: second English edition. *Dev. Environ.*
575 *Model*. 1998; 20
- 576 39. Louca S, Jacques SMS, Pires APF, Leal JS, González AL, Doebeli M, Farjalla VF.
577 Functional structure of the bromeliad tank microbiome is strongly shaped by local
578 geochemical conditions. *Environ Microbiol*. 2017; 19(8): 3132-3151
- 579 40. R Core Team. R: A language and environment for statistical computing. R Foundation
580 for Statistical Computing, Vienna, Austria. URL <https://www.R-project.org/>.2019
- 581 41. Shen H, Jiang G, Wan X, Li H, Qiao Y, Thrush S, He P. Response of the microbial
582 community to bioturbation by benthic macrofauna on intertidal flats. *J Exp Mar Biol Ecol*.
583 2017; 488, 44-51.
- 584 42. Bharagava RN, Purchase D, Saxena G, and Mulla SI. Applications of Metagenomics in
585 Microbial Bioremediation of Pollutants. *Microbial Diversity in the Genomic Era*. 2019;
586 459-477.

- 587 43. Deng J, Yin Y, Zhu W, Zhou Y. Variations in Soil Bacterial Community Diversity and
588 Structures Among Different Revegetation Types in the Baishilazi Nature Reserve. *Front.*
589 *Microbiol.* 2018; 9: 2874
- 590 44. Deng J, Zhang Y, Yin Y, Zhu X, Zhu W, Zhou Y. Comparison of soil bacterial
591 community and functional characteristics following afforestation in the semi-arid
592 areas. *PeerJ.* 2019; 7: e7141
- 593 45. Bodelier PLE. Interactions between oxygen-releasing roots and microbial processes in
594 flooded soils and sediments. In: de Kroon H, Visser EJW (eds) *Root ecology. Ecological*
595 *studies Vol. 168.* Springer-Verlag Berlin Heidelberg, Germany. 2003; 331-362
- 596 46. Carvalho PN, Araujo JL, Mucha AP, Basto MC, Almeida CM. Potential of constructed
597 wetlands microcosms for the removal of veterinary pharmaceuticals from livestock
598 wastewater. *Bioresour Technol.* 2013; 134: 412-416.
- 599 47. Chen ZJ, Shao Y, Li YJ, Lin LA, Chen Y, Tian W, Li BL, Li YY. Rhizosphere Bacterial
600 Community Structure and Predicted Functional Analysis in the Water-Level Fluctuation
601 Zone of the Danjiangkou Reservoir in China During the Dry Period. *Int J Environ Res*
602 *Public Health.* 2020; 17(4): 1266.
- 603 48. Zhang XY, Wang ZZ, Liu XY, Hu X. Degradation of diesel pollutants in Huangpu-
604 Yangtze River estuary wetland using plant-microbe systems. *Int Biodeterior*
605 *Biodegradation.* 2013; 76: 71e75.
- 606 49. Zou J, Liu X, He C, Zhang X, Zhong C, Wang C, Wei J. Effect of *Scripus triqueter* of its
607 rhizosphere and root exudates on microbial community structure of simulated diesel-
608 spiked wetland. *Int Biodeterior Biodegradation* 2013; 82: 110-116.

- 609 50. Thomas JC, Cable E, Dabkowski RT, Gargala S, McCall D, Pangrazzi G, Pierson A,
610 Ripper M, Russell DK, Rugh CL. Native Michigan plants stimulate soil microbial species
611 changes and PAH remediation at a legacy steel mill. *Int J Phytoremediation*. 2012; 15: 5-
612 23
- 613 51. Nguyen NL, Kim YJ, Hoang VA, Subramaniam S, Kang JP, Kang CH, Yang DC
614 Bacterial Diversity and Community Structure in Korean Ginseng Field Soil Are Shifted
615 by Cultivation Time. *PLOS One*. 2016; 11(5), e0155055.
- 616 52. Zhang B, Li Y, Xiang SZ, Yan Y, Yang, R, Lin MP, Wang XM, Xue YL, Guan XY.
617 Sediment Microbial Communities and Their Potential Role as Environmental Pollution
618 Indicators in Xuande Atoll, South China Sea. *Front Microbiol*. 2020; 11:1011.
- 619 53. Song W, Qi R, Zhao L, Xue N, Wang L, Yang Y. Bacterial community rather than metals
620 shaping metal resistance genes in water, sediment and biofilm in lakes from arid
621 northwestern China. *Environ Pollut*. 2019. 254: 113041.
- 622 54. Zhang S, Pang S, Wang P, Wang C, Guo C, Addo FG, Li Y Responses of bacterial
623 community structure and denitrifying bacteria in biofilm to submerged macrophytes and
624 nitrate. *Sci. Rep*. 2016; 6(1): 36178
- 625 55. Faulwetter JL, Gagnon V, Sundberg C, Chazarenc F, Burr, MD, Brisson, J, Camper AK,
626 Stein OR. Microbial processes influencing performance of treatment wetlands: a review.
627 *Ecol. Eng*. 2009; 35: 987-1004.
- 628 56. Ki BM, Huh IA, Choi JH, Cho KS Relationship of nutrient dynamics and bacterial
629 community structure at the water-sediment interface using a benthic chamber experiment.
630 *J. Environ. Sci. Health A*. 2018; 53(5): 482-491.

- 631 57. Mosier AC, Francis CA. Relative abundance and diversity of ammonia-oxidizing archaea
632 and bacteria in the San Francisco Bay estuary. *Environ. Microbiol.* 2008; 10:3002-3016.
- 633 58. Vila-Costa M, Pulido C, Chappuis E, Calviño A, Casamayor EO, Gacia E. Macrophyte
634 landscape modulates lake ecosystem-level nitrogen losses through tightly coupled plant-
635 microbe interactions. *Limnol Oceanogr.* 2015; 61(1): 78-88
- 636 59. Yoon S, Cruz-García C, Sanford R, Ritalahti KM, Löffler FE Denitrification versus
637 respiratory ammonification: environmental controls of two competing dissimilatory
638 NO₃(-)/NO₂(-) reduction pathways in *Shewanella loihica* strain PV-4. *The ISME Journal.*
639 2015; 9(5):1093-1104.
- 640 60. Felföldi T, Székely AJ, Gorál R, Barkacs K, Scheirich G, András J, Márialigeti K.
641 Polyphasic bacterial community analysis of an aerobic activated sludge removing phenols
642 and thiocyanate from coke plant effluent. *Bioresour. Technol.* 2010; 101: 3406-3414.
- 643 61. Weber KA, Urrutia MM, Churchill PF, Kukkadapu RK, Roden EE. Anaerobic redox
644 cycling of iron by freshwater sediment microorganisms. *Environ Microbiol.* 2006; 8:100-
645 113.
- 646 62. Fabian M, Marrale D, Misic C. Bacteria and organic matter dynamics during a
647 bioremediation treatment of organic-rich harbor sediments. *Mar Pollut Bull.* 2003; 46:
648 1164-1173.
- 649 63. Haddad HR, Maine MA, Bonetto CA. Macrophyte growth in a pilot-scale constructed
650 wetland for industrial wastewater treatment. *Chemosphere.* 2006; 63(10): 1744-1753.
- 651 64. Wu Q, Zhang R, Huang S, Zhang H. Effects of bacteria on nitrogen and phosphorus
652 release from river sediment. *J Environ Sci.* 2008; 20: 404-412.

653 65. Sinkko H, Lukkari K, Sihvonen LM, Sivonen K, Leivuori M, Rantanen M, Paulin L,
654 Lyra C. Bacteria contribute to sediment nutrient release and reflect progressed
655 eutrophication-driven hypoxia in an organic-rich continental sea. PLOS One. 2013; 8:
656 e67061.

657

658 **Figure Legends**

659 **Fig 1** Benthic inorganic nutrient flux rates. (A) Sediment oxygen consumption- SOC and (B)
660 (Total ammonia nitrogen- TAN, nitrate, nitrite and soluble reactive phosphate- SRP) estimated
661 during laboratory incubations (mean±SD, n=3) in each treatment system

662 **Fig 2** The relative abundance of the vertical sediment microbial community composition and
663 diversity among the treatment systems (Biofilm, Constructed-wetland, Sedimentation) at the
664 phylum (A), class (B) and family (C) levels revealed by 16S rRNA genes sequencing. Taxa
665 making up less than 0.03% of total composition in all libraries were classified as ‘others’

666 **Fig 3** Alpha diversity estimates of each treatment at different sampling depths obtained by 16S
667 rRNA genes high-throughput sequencing. (A) Number of OTUs, (B) Chao1 richness estimate
668 index, (C) Shannon index and (D) Simpson

669 **Fig 4** Non-metric multidimensional scaling plot based on the Bray-Curtis dissimilarity showing
670 the relationship between the samples in each treatment. Shapes in triangle, circles, and squares
671 represent biofilm, constructed-wetland, and sedimentation treatments respectively. Colors in
672 brown, blue and green represent samples at the surface, middle and bottom sediment depth in
673 each system respectively

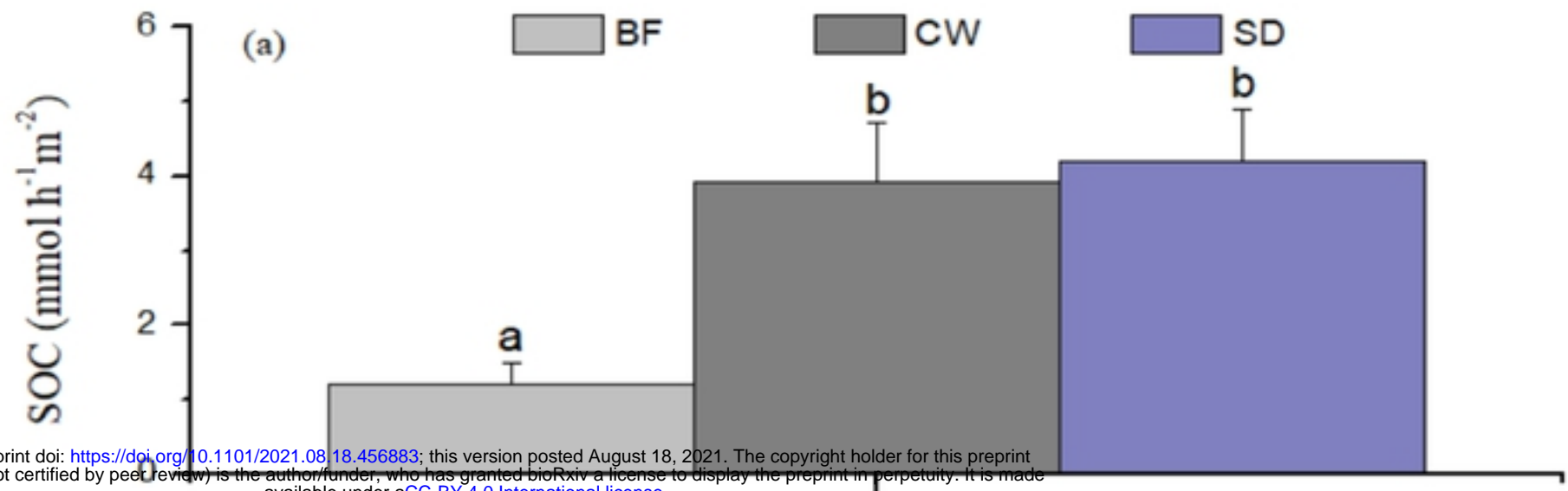
674 **Fig 5** Canonical Correspondence Analysis ordination plot showing the relationships between
675 bacterial community and physicochemical variables in the three treatments of the aquaculture

676 tail-water treatment system. Samples collected from the surface, middle, and bottom of each
677 system are designated with blue, orange, and green triangles, respectively. The abbreviations
678 indicate sediment oxygen consumption (SOC), total- organic matter (TOM), organic nitrogen
679 (TON), ammonia nitrogen (TAN), phosphate (TP), nitrate (NO_3^- -N), nitrite (NO_2^- -N) and
680 sediment reactive phosphate (SRP)

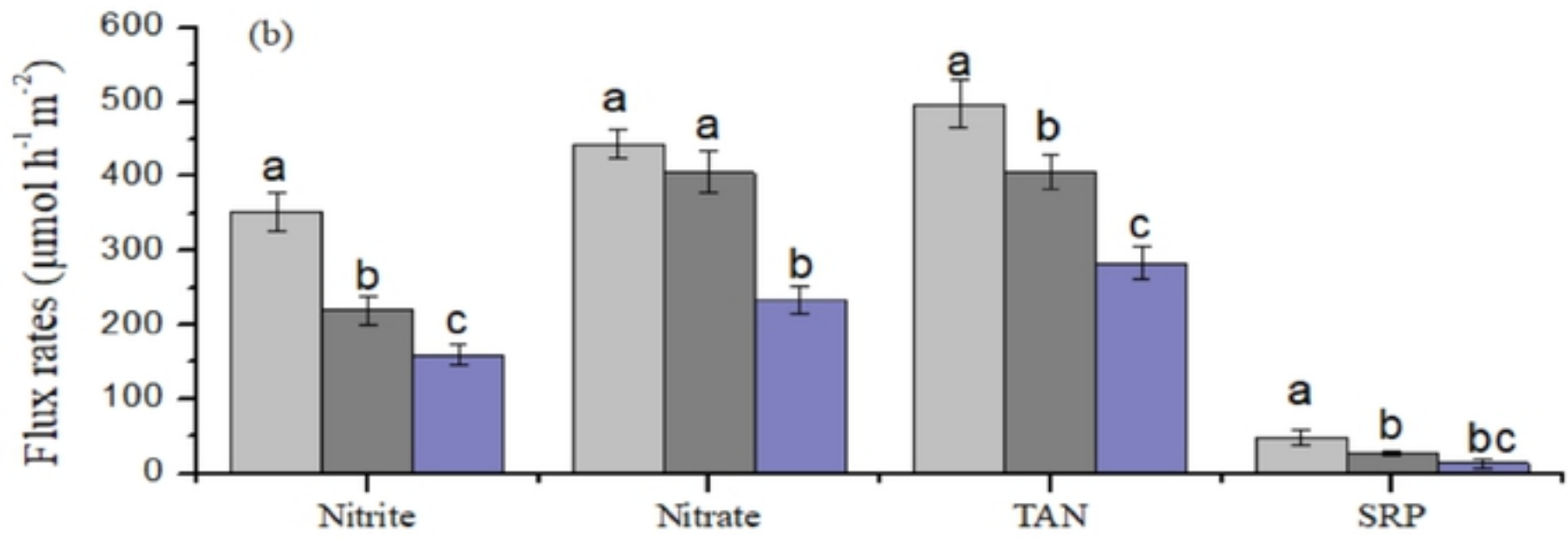
681 **Fig 6** Bar plot of the relative abundance distributions of the predicted predominant functional
682 groups among the treatments as annotated by the FAPROTAX database.

1 **Figures**

2



bioRxiv preprint doi: <https://doi.org/10.1101/2021.08.18.456883>; this version posted August 18, 2021. The copyright holder for this preprint (which was not certified by peer review) is the author/funder, who has granted bioRxiv a license to display the preprint in perpetuity. It is made available under aCC-BY 4.0 International license.



3

4

[Fig 1]

5

6

bioRxiv preprint doi: <https://doi.org/10.1101/2021.08.18.456883>; this version posted August 18, 2021. The copyright holder for this preprint (which was not certified by peer review) is the author/funder, who has granted bioRxiv a license to display the preprint in perpetuity. It is made available under aCC-BY 4.0 International license.

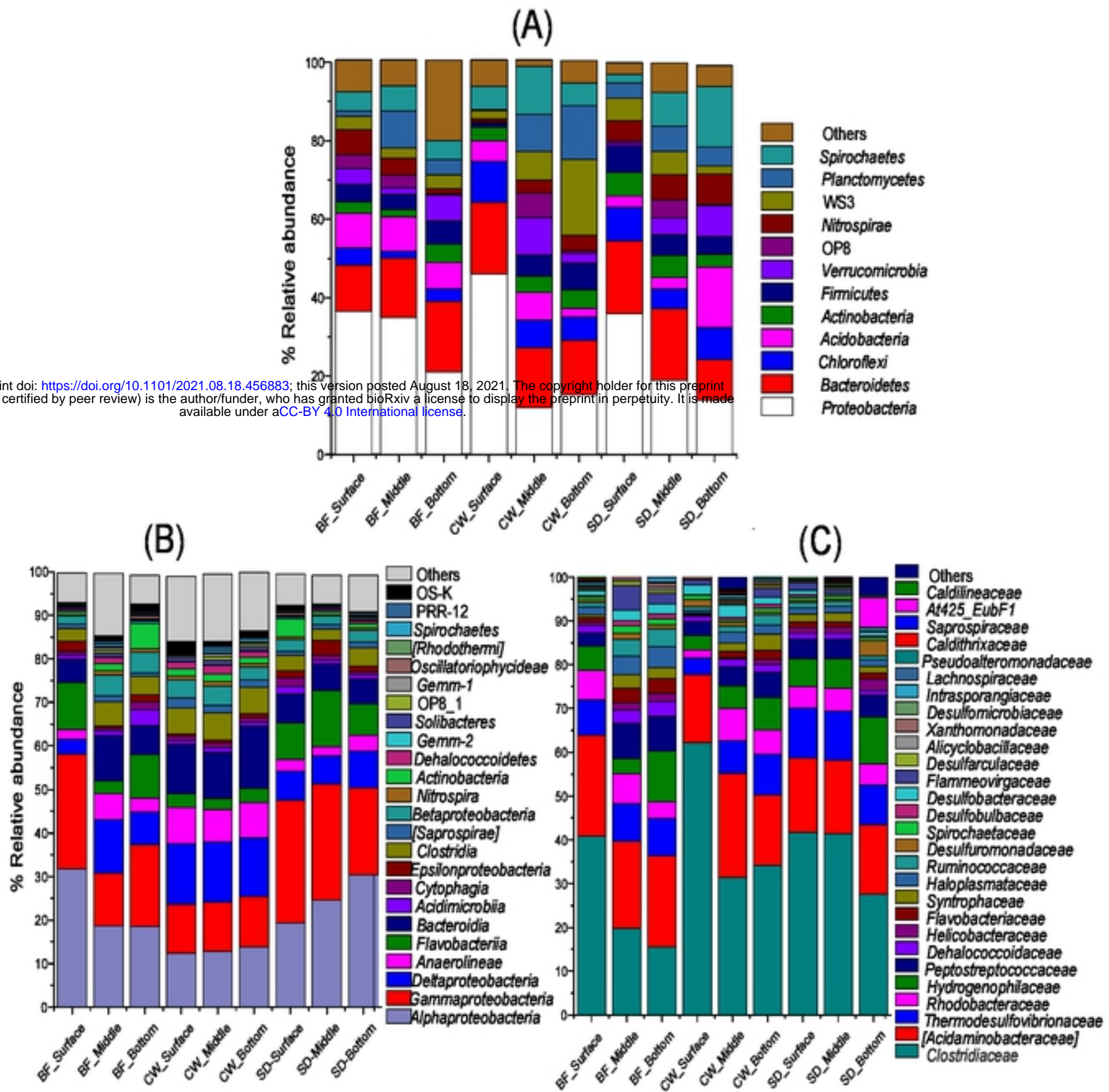
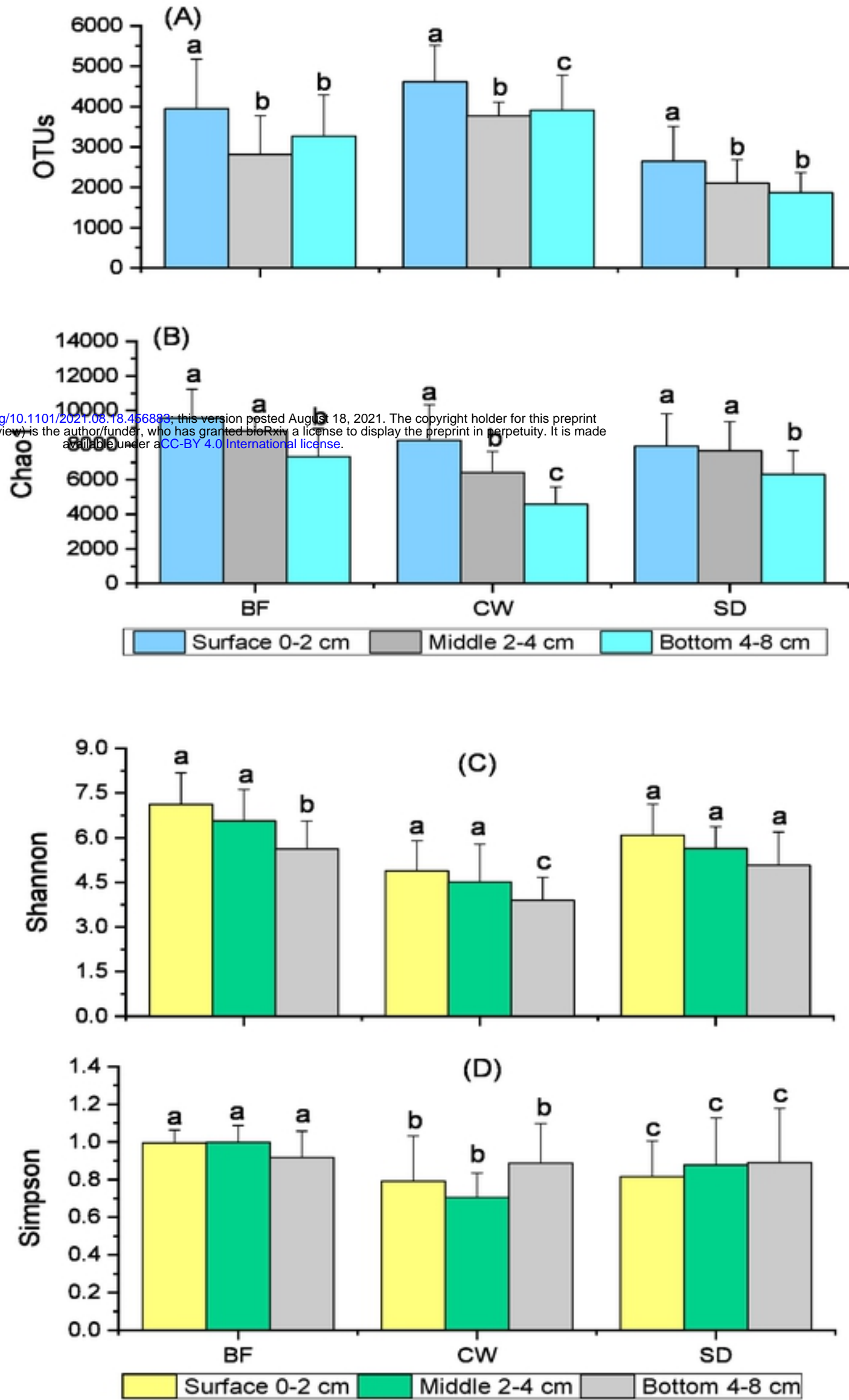


[Fig 2]

bioRxiv preprint doi: <https://doi.org/10.1101/2021.08.18.456899>; this version posted August 18, 2021. The copyright holder for this preprint (which was not certified by peer review) is the author/funder, who has granted bioRxiv a license to display the preprint in perpetuity. It is made available under aCC-BY 4.0 International license.



12

13

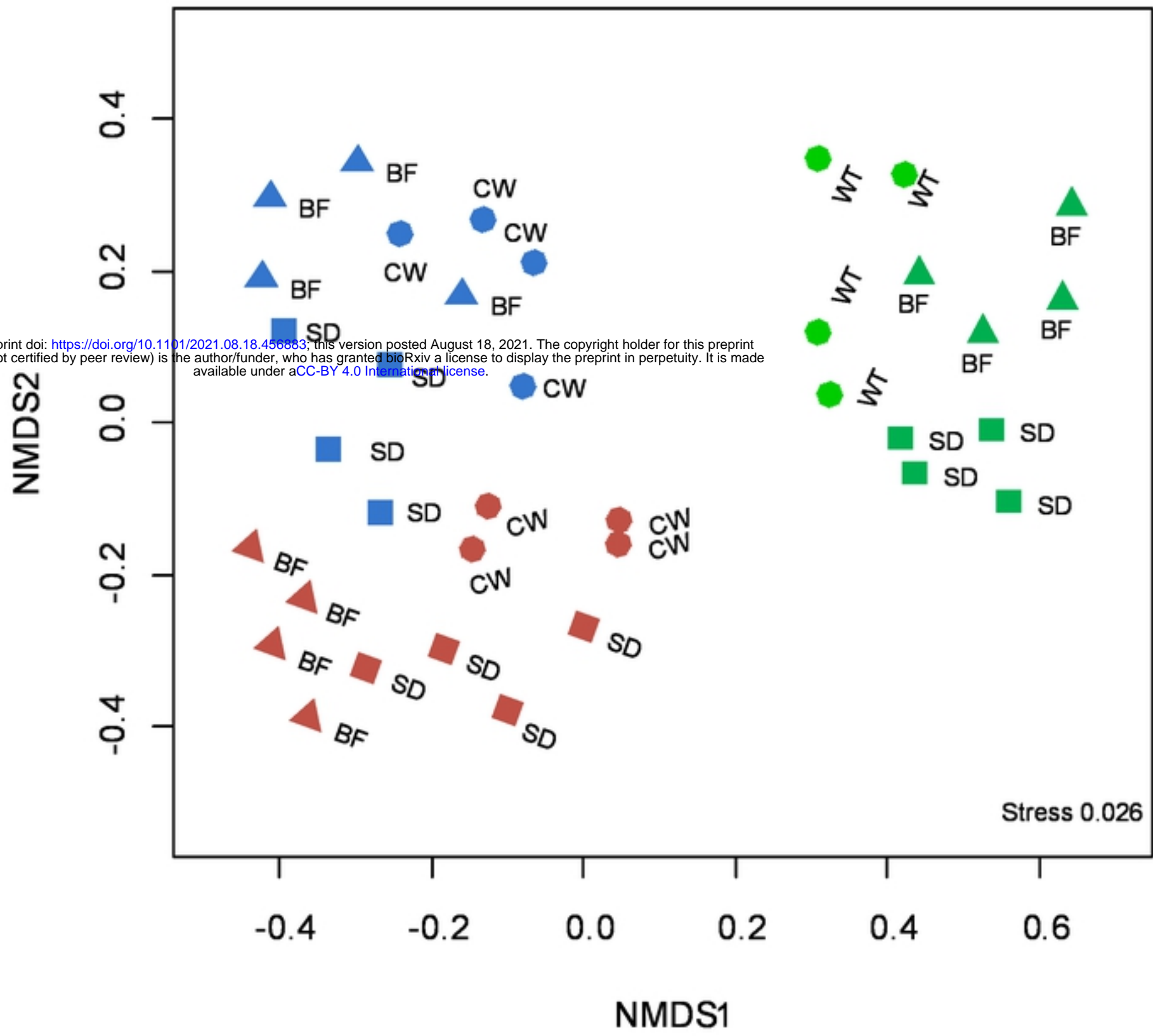
14

[Fig 3]

15

16

bioRxiv preprint doi: <https://doi.org/10.1101/2021.08.18.456883>; this version posted August 18, 2021. The copyright holder for this preprint (which was not certified by peer review) is the author/funder, who has granted bioRxiv a license to display the preprint in perpetuity. It is made available under aCC-BY 4.0 International license.

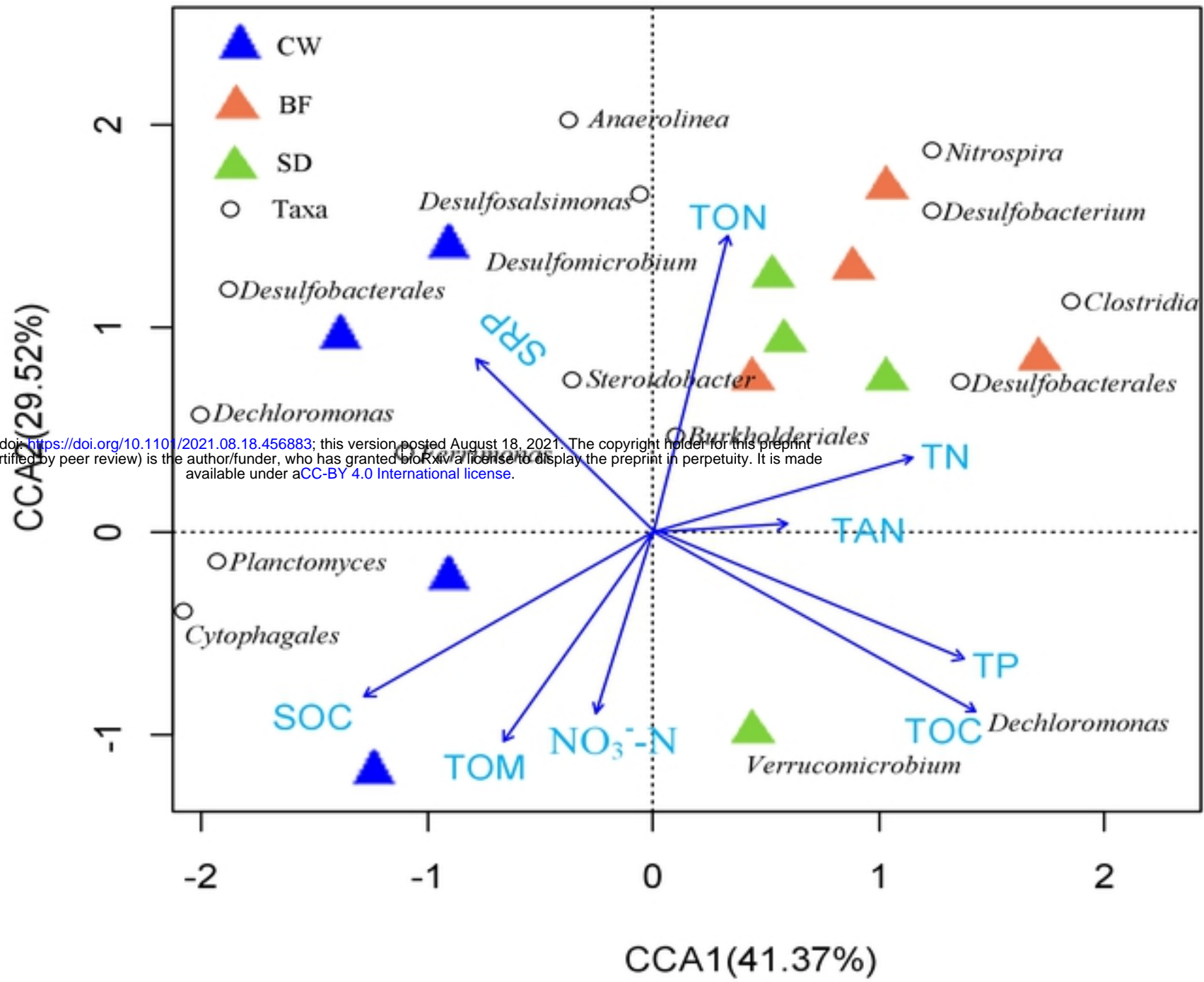


17

18

19

[Fig 4]



bioRxiv preprint doi: <https://doi.org/10.1101/2021.08.18.456883>; this version posted August 18, 2021. The copyright holder for this preprint (which was not certified by peer review) is the author/funder, who has granted bioRxiv a license to display the preprint in perpetuity. It is made available under aCC-BY 4.0 International license.

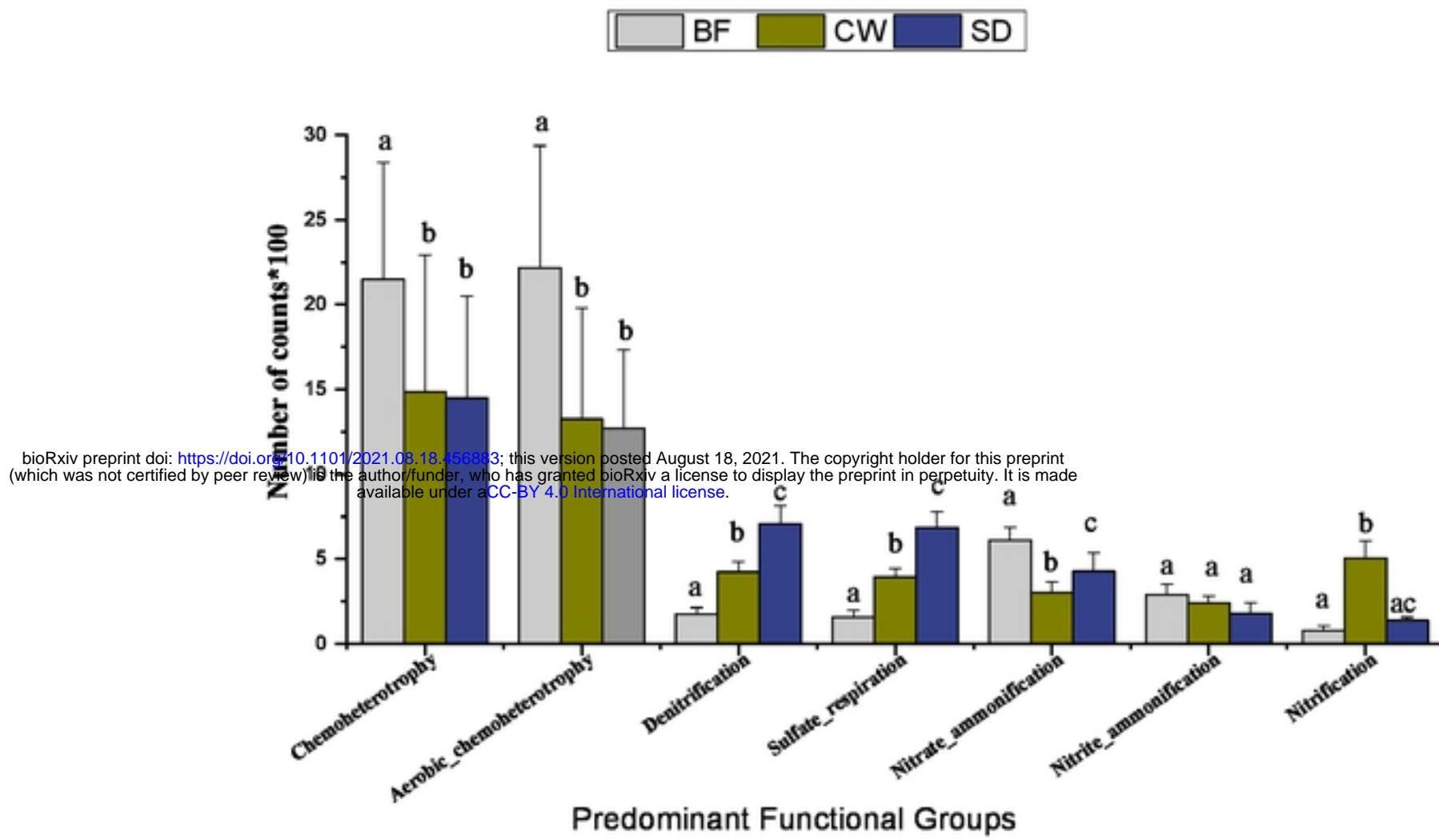
21

22

23

24

[Fig 5]



26

27

28

[Fig 6]